Reduced histone biosynthesis and chromatin changes arising from a damage signal at telomeres

Roderick J. O'Sullivan[1], Stefan Kubicek [2], Stuart L. Schreiber [2,3,4,] and Jan Karlseder[1, 5]

[1]The Salk Institute for Biological Studies

Molecular and Cellular Biology Department

10010 North Torrey Pines Rd.

La Jolla, CA92037

USA

[2]The Broad Institute of Harvard and MIT, 7 Cambridge Center, Cambridge, MA02142, USA

[3]Howard Hughes Medical Institute, Harvard University, 7 Divinity Avenue, Cambridge, MA 02138, USA

[4]Department of Chemistry and Chemical Biology, Harvard University, 7 Divinity Avenue, Cambridge, MA 02138, USA

[5] To whom correspondence should be addressed

Email: Karlseder@salk.edu

Phone: 858 453 4100 x1867

Fax: 858 457 4765

Supplementary Fig. 1
O'Sullivan et al. 2010

a PI Staining

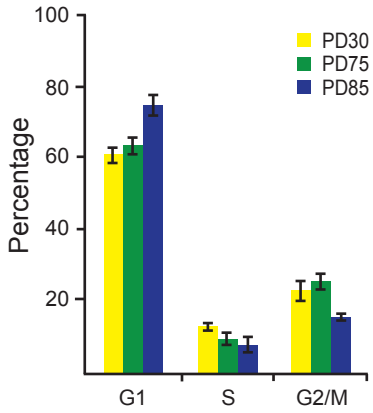

b H3pS10

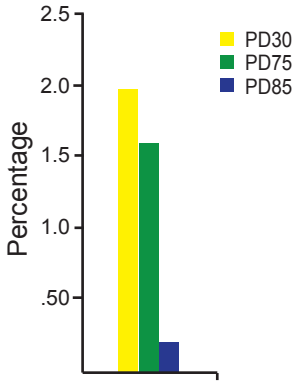

c BrdU

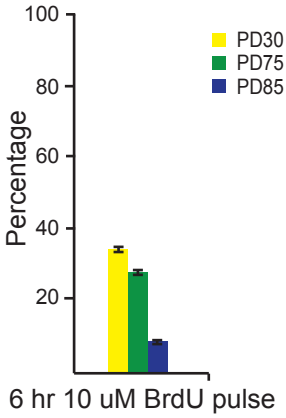

d

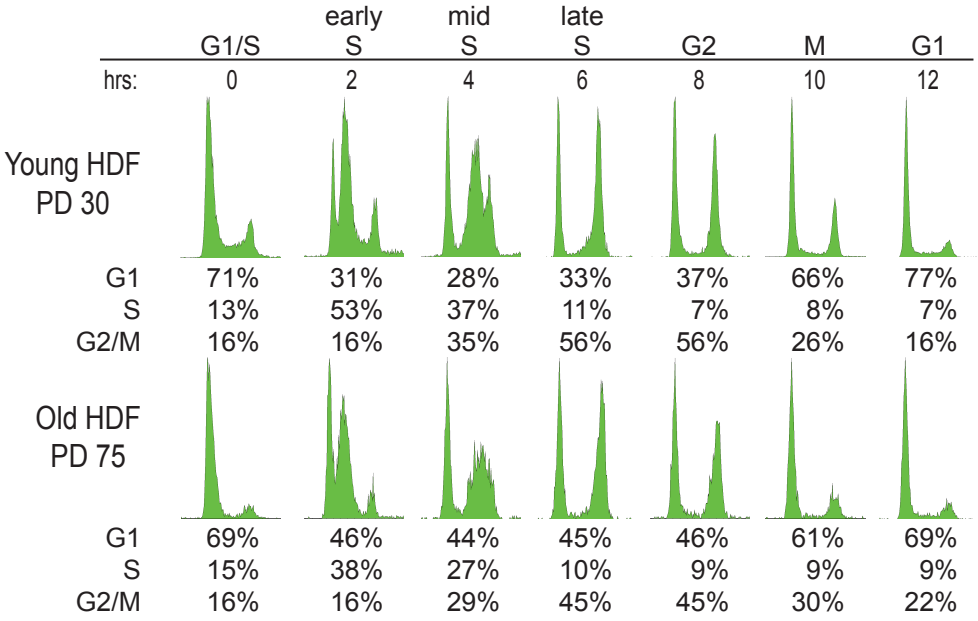

e

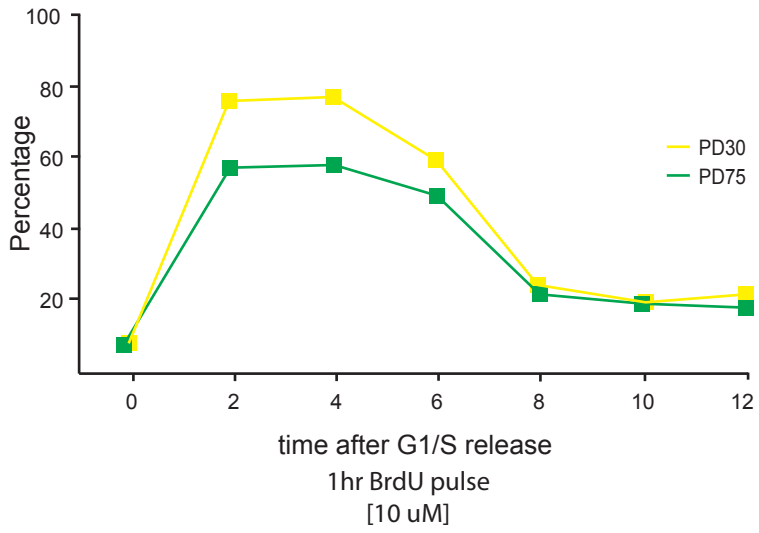

Supplementary Figure 1 Similar cell cycle dynamics of early and late passage fibroblast populations (**a**) Histone H3 and H4 expression of IMR90, IMR90 expressing HPV16 E6 and E7, HCT116 with functional p53 and HCT116 without a p53 allele. Cells were subjected to 6 days of 500ng/ml of bleomycin where indicated. Error bars represent the standard deviation of three independent experiments. (**b**) Histone H3 serine 10 phosphorylation was determined by FACS analysis in populations of PD30, PD75 and senescent IMR90 lung fibroblasts. The percentages of H3S10ph positive cells are indicated. (**c**) BrdU incorporating fractions from populations of PD30, PD75 and senescent IMR90 lung fibroblasts have been determined by FACS. The percentages of BrdU positive cells are indicated. Error bars represent the standard deviation of three independent experiments. (**d**) FACS analysis to monitor cell cycle progression following release from thymidine-aphidicolin G1/S block. Indicated above each plot is the cell cycle phase as extrapolated from measurement of DNA content according to PI staining at each time point. Percentages of cells in each cell cycle phase are indicated below the FACS diagrams. (**e**) BrdU incorporation profiles of PD30 and PD75 IMR90 populations at 2 hour intervals. The percentage of BrdU incorporating cells and hours after G1/S release are indicated.

Supplementary Fig. 2
O'Sullivan et al. 2010

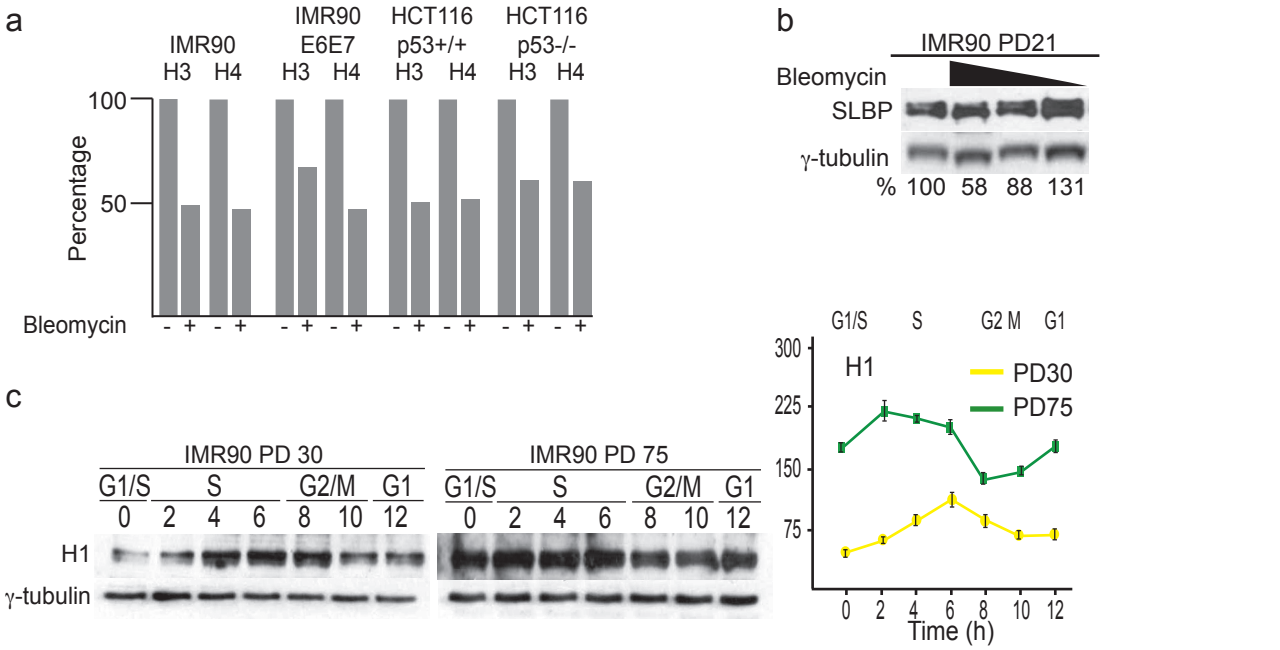

Supplementary Figure 2 H3 and H4 expression respond to DNA damage. (**a**) H3 and H4 expression (%) in IMR90, IMR90 expressing HPV16 E6 and E7, HCT116 cells expressing wild type p53 and HCT116 cells deleted for p53. The cultures have been grown in the presence of 500ng/ml bleomycin where indicated. (**b**) Expression of SLBP in IMR90 fibroblasts treated for 6 days with 500, 50 or 5 ng/ml of Bleomycin. γ-tubulin serves as a loading control. The percent expression change of two independent experiments has been indicated. (**c**) Cell cycle expression of H1 in PD30 and PD75 HDFs. Hours after G1/S release are indicated and corresponding cell cycle phases have been determined by FACS analysis. γ-tubulin serves as loading control. Quantifications of cell cycle expression patterns of H1 from PD30 (yellow lines) and PD75 (green lines) are shown on the right. Cell cycle phases are indicated on top and hours after release from G1/S on the bottom. Corresponding cell cycle phases have been determined by FACS analysis. The error bars represent the standard deviation of three independent experiments. (**d**) Hoechst 33342 incorporating cells were sorted from early and late passage IMR90 populations. Gates used for sorting and isolation of pure G1 and S/G2/M populations have been indicated. (**e**) Analysis of H3, H3K79me2, H4, H4K5Ac, and H4K20me2 expression in G1 phase and S/G2/M phase fractions of cycling early and late passage IMR90 cells. Expression levels were normalized to γ–tubulin loading control and indicated in arbitrary units. (**f**) H3K56ac, H3K79me2 and H4K20me2 in early passage IMR90 HDFs treated for 6 days with 500, 50 and 5ng/ml of bleomycin. Error bars represent the standard deviation of three independent experiments.

Supplementary Fig. 3
O'Sullivan et al. 2010

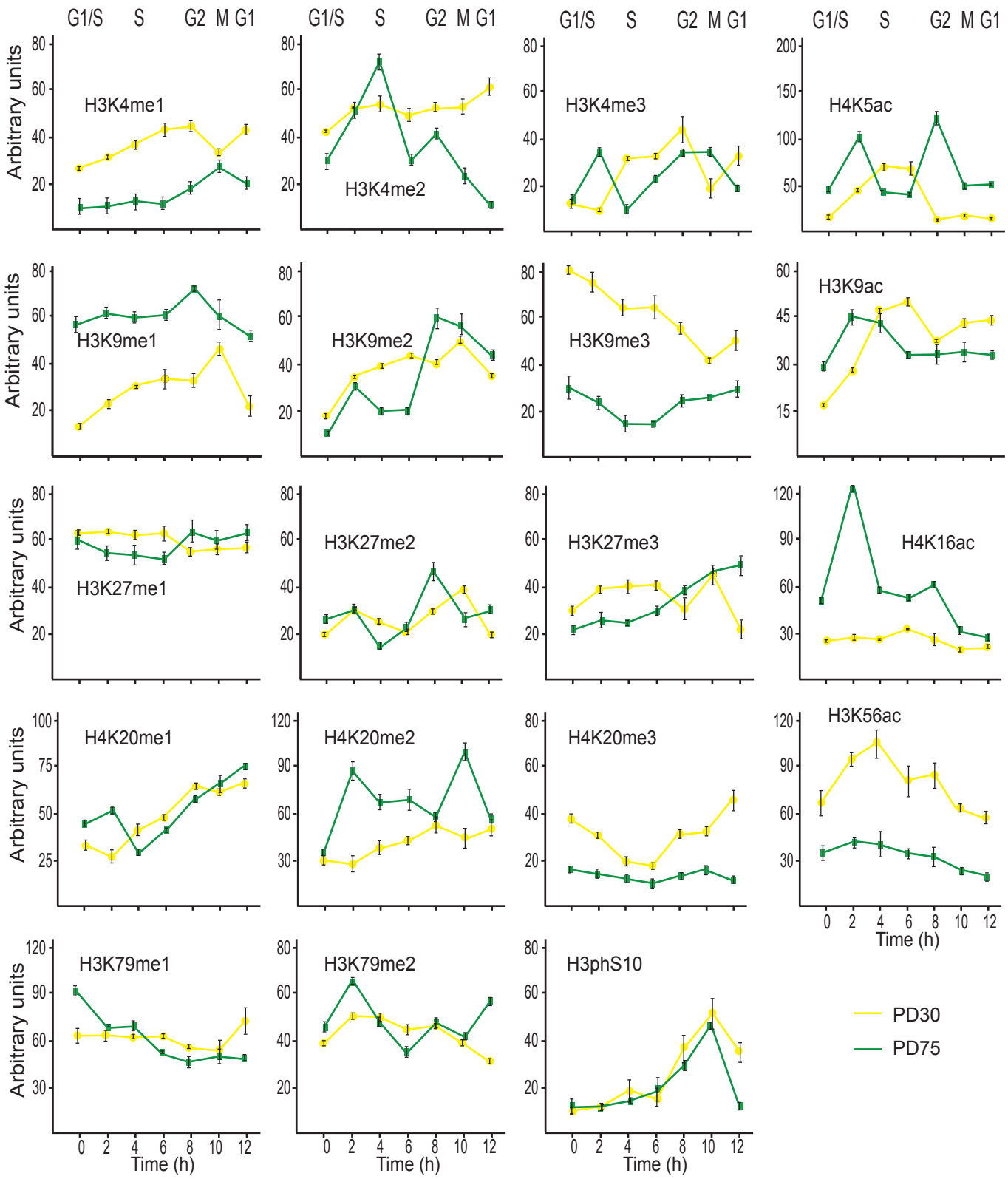

Supplementary Figure 3 Altered redistribution of epigenetic marks upon cellular aging. Quantifications of cell cycle distribution of histone modifications in whole cell extracts from PD30 (yellow lines) and PD75 (green lines) HDFs. Shown are cell cycle patterns of H3K4me1/2/3, H4K5Ac, H3K9me1/2/3, H3K9Ac, H3K27me1/2/3, H4K16Ac, H4K20me1/2/3, H3K56ac, H3S10ph, H3K79me1/2 and H3phS10. Enrichments were calculated relative to corresponding core histones. Cell cycle phases are indicated on top and hours after release fromG1/S on the bottom. Corresponding cell cycle phases have been determined by FACS analysis. The error bars represent the standard deviation of three independent experiments.

Supplementary Fig. 4
O'Sullivan et al. 2010

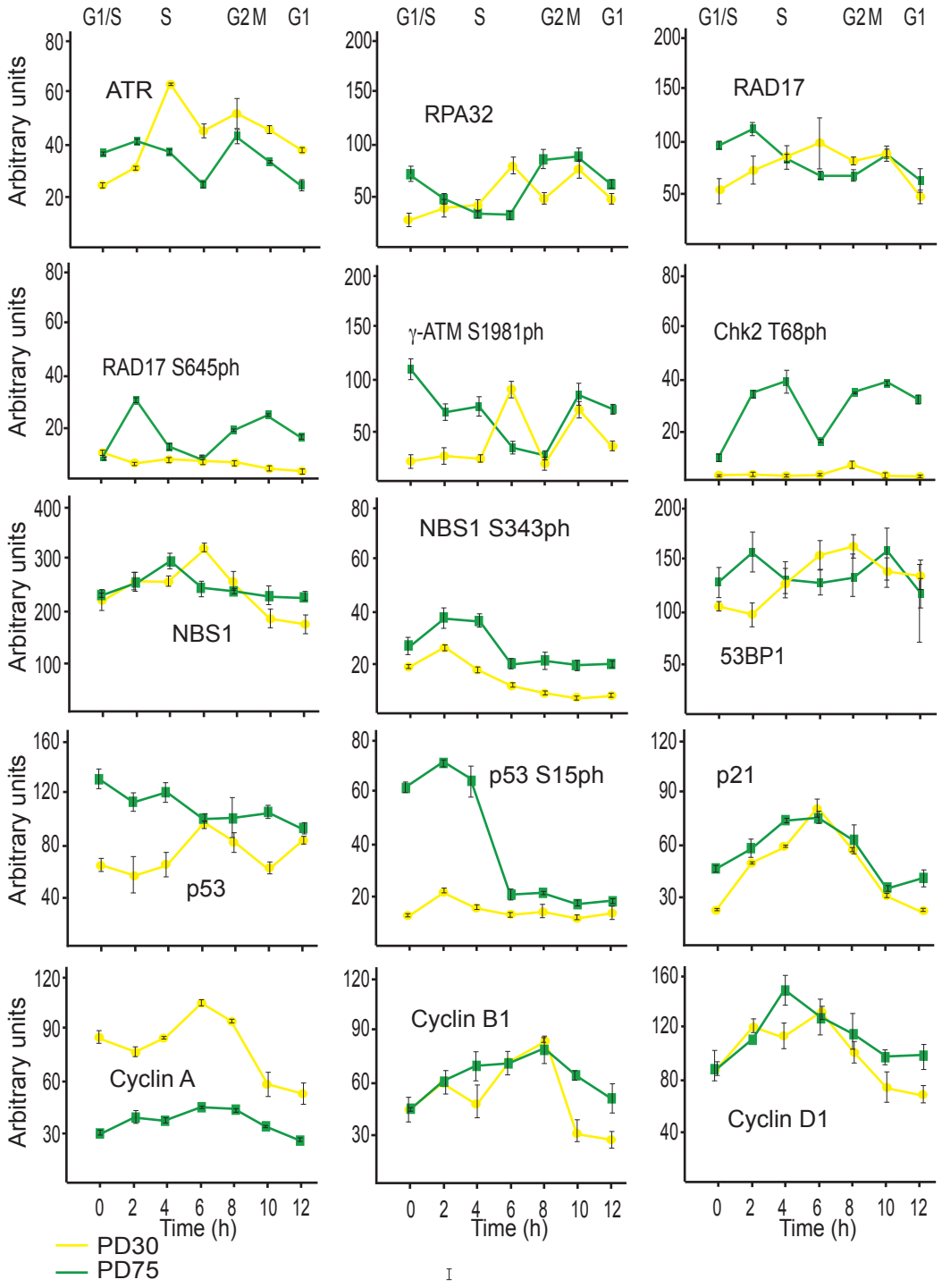

Supplementary Figure 4 DNA damage accumulation and DDR activation upon cellular aging. Quantification of expression of PCNA, Rpa32, Rad51, ATR, Rad17, Rad17-pS645, γ-ATM pS1981, Chk2-pT68, NBS1, NBS1S343ph, 53BP1, p53, p53S15ph, p21 and Cyclins A/B1D1 in whole cell extracts of PD30 (yellow lines) and PD75 (green lines) HDFs. Expression levels were calculated relative to γ-tubulin. Corresponding cell cycle phases have been determined by FACS analysis and are indicated on top and hours after release from G1/S on the bottom. The error bars represent the standard deviation of three independent experiments.

Supplementary Fig. 5
O'Sullivan et al. 2010

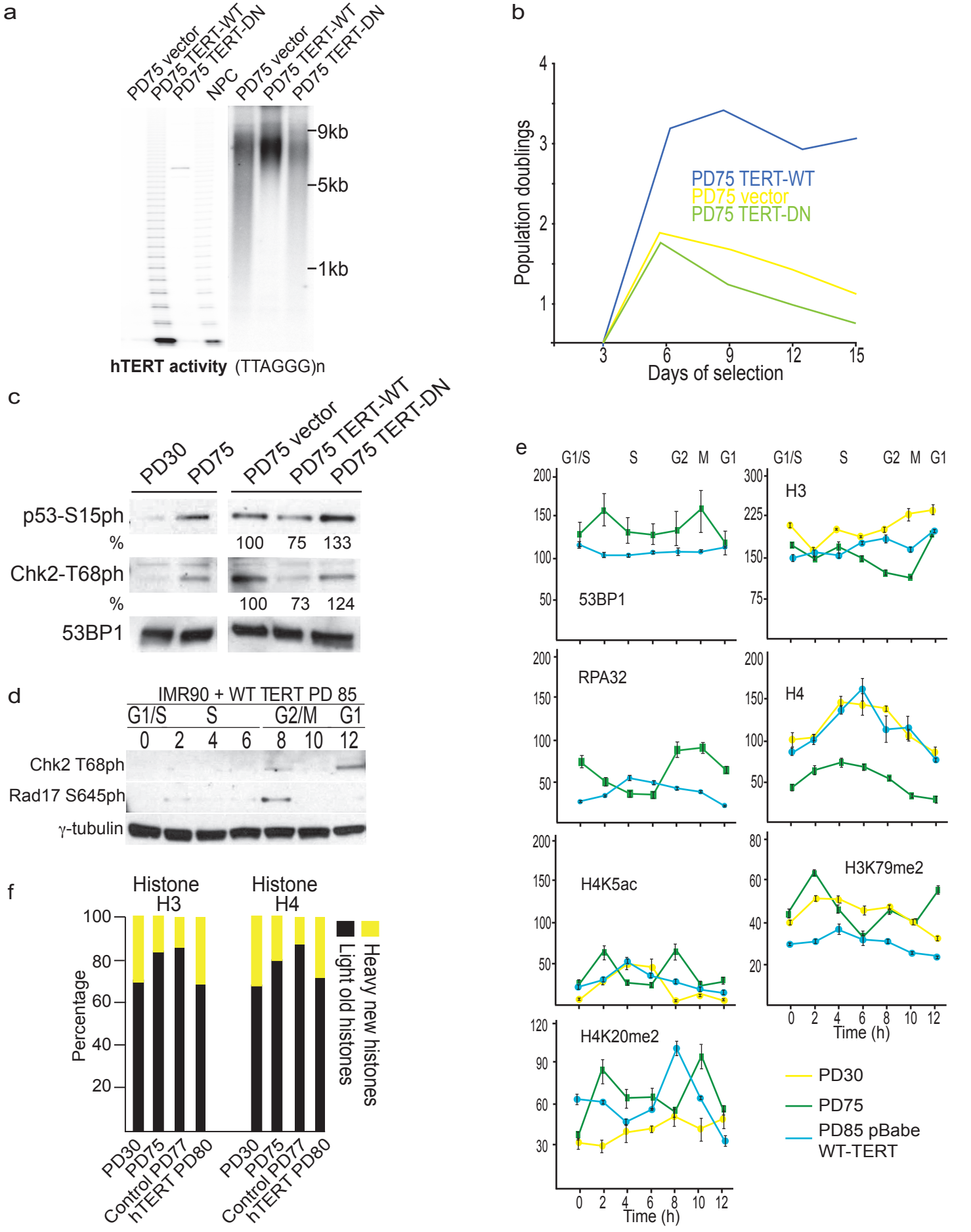

Supplementary Figure 5 Expression of hTERT in PD75 IMR90 fibroblasts. (**a**) Telomerase activity and telomere length in PD75 IMR90 fibroblasts, PD75 cells expressing wild type hTERT (TERT-WT), PD75 cells expressing dominant negative hTERT (TERT-DN). Neuronal precursor stem cell (NPC) nuclear extract served as positive control for telomerase activity. (**b**) Proliferation curves of IMR90 fibroblasts expressing wild type hTERT, a control vector of dominant negative hTERT. (**c**) Expression of p53-S15ph, Chk2-T68ph and 53BP1 in young PD30, old PD75 and PD75 cells expressing wild type hTERT (TERT-WT), PD75 cells expressing dominant negative hTERT (TERT-DN). The percentile of p53S15ph and CHK2 T68ph in relation to γ-tubulin is indicated. (**d**) Expression of Chk2-pT68 and Rad17-pS645 in whole cell extracts of PD85 cells expressing hTERT. 75,000 cell equivalents were loaded per lane and equal loading was confirmed by ponceau staining prior to probing with primary antibodies. Hours after G1/S release are indicated and corresponding cell cycle phases have been determined by FACS analysis and indicated. γ-tubulin serves as loading control. (**e**) Quantification of expression of 53BP1, Rpa32, H3, HrK79me2, H4, H4K5ac and H4K20me2 in whole cell extracts of early passage HDFs (yellow lines), late passage HDFs (PD75, green lines) and of late passage HDFs expressing catalytically active hTERT (PD85, blue lines). Expression levels were calculated relative to γ-tubulin. Corresponding cell cycle phases have been determined by FACS analysis and are indicated on top and hours after release from G1/S on the bottom. The error bars represent the standard deviation of three independent experiments. (**f**) SILAC labeling of PD30, PD75, PD77 (control) and PD80

(hTERT expressing) HDFs and mass spectroscopy of histone proteins. Shown are percentages of newly synthesized histones (yellow) and histones from previous cell cycle (black).

Supplementary Fig. 6
O'Sullivan et al. 2010

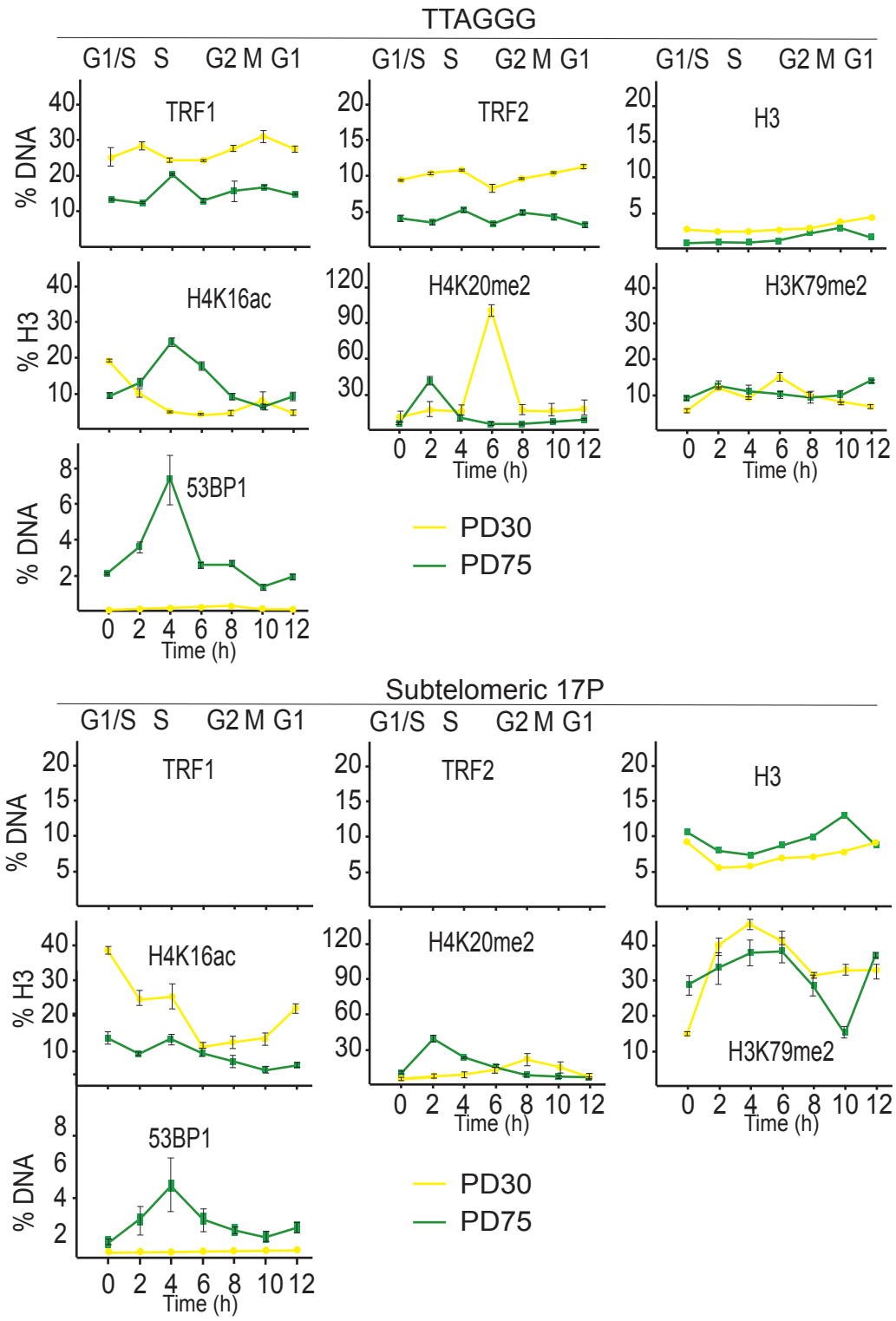

Supplementary Figure 6 Telomeric and subtelomeric histone modifications upon cellular aging. Quantifications of cell cycle distribution of histone modifications at telomeres and 17P in PD30 (yellow lines) and PD75 (green lines) HDFs. Shown are cell cycle binding patterns of TRF1, TRF2, H3, H4K16Ac, H4K20me2, H3K79me2, and 53BP1 as determined by ChIP. Cell cycle phases are indicated on top and hours after release from G1/S on the bottom. Corresponding cell cycle phases have been determined by FACS analysis. The error bars represent the standard deviation of three independent experiments.

Supplementary Table 1

Antibody	Source/Company	Cat #	Lot #	Reference
H3	Abcam	1791	494671	
H4	Abcam	7311	627417	
H2A	Active Motif	39209		
H2B	Active Motif	39125		
SLBP	Sigma/Aldrich	WH0007884M1		
H3K4me1	Upstate/Millipore	07-436		
H3K4me2	Upstate/Millipore	07-030		
H3K4me3	Upstate/Millipore	05-745		
H3K9me1, me2	Thomas Jenuwein			20
H3K9me3	Thomas Jenuwein			20
H3K9me3	Abcam	8988	638466	
H3K9me3	Active Motif	39161	170	
H3K9ac	Abcam	4441		
H3S10 ph	Upstate/Millipore	06-570	32219	
H3K27me1, me2, me3	Thomas Jenuwein			20
H3K79me1	Active Motif	39146	172	
H3K79me2	Abcam	3594	621252	
H4K5ac	Serotec	AHP962	251105	
H4K16ac	Abcam			
	Active Motif	23352	107	
	Upstate/Millipore	07-329	JBC1355136	
H3K56ac	Upstate/Millipore	07-677	JBC1361855	
H4K20me1	Thomas Jenuwein	0077		57
	Active Motif	39539	01008001	
H4K20me2	Thomas Jenuwein	0080		57
H4K20me3	Thomas Jenuwein	0083		57
53BP1 (H-300)	Santa Cruz	22760	J2507	
Asf1a/b	Genevieve Almouzni			3,38
SLBP	Sigma	WH0007884M1		
ATM	Bethyl	A300-299A	A2	
ATM S1981 ph	Rockland	200-301-400	20772	
ATR	Abcam	10312	534864	
BrdU	Bd Biosciences	347580		
CAF1 p150	Abcam	7655	683997	
CAF1 p60	Bethyl	A201-085A	A1	
Chk2 T68 ph	CST	2661		
Cyclin A, B1, D1	Tony Hunter			58
HP1α	Upstate/Millipore	MAB3446		
HP1γ	Upstate/Millipore	MAB3450		
p21	Upstate/Millipore	05-655	27757	
p53 (DO1)	Santa Cruz	126	H2707	
p53 S15 ph	CST	9254	9	
PCNA	Santa Cruz	7907	H1605	
RAD17 (H-300)	Santa Cruz	5613	K1904	
RAD17 S645 ph	CST	3421	2	
RAD51 (H92)	Santa Cruz	8349	8349	
RPA32	Abcam	2175	314161	
TRF1, 2	Karlseder Lab	6840		55
γ–Tubulin	Sigma-Aldrich	GTU-88		

Supplementary References.

57. Martens, J.H. et al. The profile of repeat-associated histone lysine methylation states in the mouse epigenome. *EMBO J* **24**, 800-12 (2005).
58. Pines, J. & Hunter, T. Human cyclins A and B1 are differentially located in the cell and undergo cell cycle-dependent nuclear transport. *J Cell Biol* **115**, 1-17 (1991).